Quantum funneling in blended multi-band gap core/shell colloidal quantum dot solar cells

Darren C. J. Neo, Samuel D. Stranks, Giles E. Eperon, Henry J. Snaith, Hazel E. Assender, and Andrew A. R. Watt

Citation: Applied Physics Letters **107**, 103902 (2015); doi: 10.1063/1.4930144
View online: http://dx.doi.org/10.1063/1.4930144
View Table of Contents: http://scitation.aip.org/content/aip/journal/apl/107/10?ver=pdfcov
Published by the AIP Publishing

Quantum funneling in blended multi-band gap core/shell colloidal quantum dot solar cells

Darren C. J. Neo,[1] Samuel D. Stranks,[2] Giles E. Eperon,[2] Henry J. Snaith,[2] Hazel E. Assender,[1] and Andrew A. R. Watt[1,a)]
[1]*Department of Materials, University of Oxford, 16 Parks Road, OX1 3PH Oxford, United Kingdom*
[2]*Department of Physics, Clarendon Laboratory, Parks Road, OX1 3PU Oxford, United Kingdom*

(Received 18 December 2014; accepted 24 August 2015; published online 10 September 2015)

Multi-band gap heterojunction solar cells fabricated from a blend of 1.2 eV and 1.4 eV PbS colloidal quantum dots (CQDs) show poor device performance due to non-radiative recombination. To overcome this, a CdS shell is epitaxially formed around the PbS core using cation exchange. From steady state and transient photoluminescence measurements, we understand the nature of charge transfer between these quantum dots. Photoluminescence decay lifetimes are much longer in the PbS/CdS core/shell blend compared to PbS only, explained by a reduction in non-radiative recombination resulting from CdS surface passivation. PbS/CdS heterojunction devices sustain a higher open-circuit voltage and lower reverse saturation current as compared to PbS-only devices, implying lower recombination rates. Further device performance enhancement is attained by modifying the composition profile of the CQD species in the absorbing layer resulting in a three dimensional quantum cascade structure. © *2015 AIP Publishing LLC*.
[http://dx.doi.org/10.1063/1.4930144]

Lead sulfide (PbS) colloidal quantum dots (CQDs) are candidate absorber materials for a new generation of low cost, solution-processed solar cells.[1,2] The ability to tune the band gap across the solar spectrum through quantum confinement allows the possibility to create broadband multi-junction and multi-band gap solar cells.[3] If this can be harnessed alongside multiple exciton generation[4] and emerging energy transfer mechanisms[5] there is a very real opportunity to break the Shockley Queisser limit.[6] However, realizing this possibility has proven challenging to date due to poor current matching and mismatched energy levels in tandems and charge recombination losses in multi-band gap structures.[7,8]

One of the first attempts to couple different layers of CQD with different band gaps was by Klar *et al*. in 2005, who fabricated a cascaded band gap multilayer structure using light-emitting CQD and demonstrated efficient funneling of excitons from large to small band gap.[9] Xu *et al*. used photoluminescence (PL) techniques to show that the efficiency of charge transfer between small and large band gap PbS CQD could be enhanced by chemically cross-linking ligands.[10] The first multi-band gap cascaded CQD solar cell that performed better than a single band gap reference device was produced by Kramer *et al*., who improved charge extraction by modifying the depletion region using a graded band-gap structure. Efficiency enhancement was largely gained through improved fill factor.[11] Similar strategies have been exploited in organic photovoltaics (OPV) to increase absorption without compromising charge extraction.[12]

Another strategy of OPV is to improve charge extraction through the formation of bulk heterojunctions where short diffusion lengths are mitigated by increasing the heterojunction's interfacial area.[13] Recently, Rath *et al*. demonstrated a CQD bulk heterojunction between *p*-type PbS CQD and *n*-type bismuth sulfide (Bi_2S_3).[14] Performance of the bulk heterojunction device triumphed over a reference bilayer heterojunction device, and this was ascribed to improved carrier lifetimes.[14] To date, blending different sized CQD to form a multi-band gap heterojunctions device has largely been unexplored due to the smaller band gap CQDs acting as recombination centres[15] and interfacial trap states[16] which limit performance. Zhitomirsky *et al*. showed that beyond 10% inclusion of larger sized PbS in a population of smaller PbS, the device open-circuit voltage (V_{oc}) would drop significantly,[17] and thus blending PbS populations of different sizes beyond that blend ratio proved to be ineffective.

To reduce non-radiative carrier recombination resulting from a bimodal CQD population, we use a core/shell CQD blend. Studies from Speirs *et al*.[18] and Lai *et al*.[19] independently showed via spectroscopic techniques that the presence of CdS shell acts to passivate traps states and reduces trap density, thereby improving carrier lifetime, while Wheeler *et al*. was able to show the reduced trap densities in PbS/CdS core/shell quantum dots as compared to PbS cores,[20] via a combination of ultra-fast absorption spectroscopy and photoluminescence. Additionally, Gonfa *et al*. demonstrated improved device performance of PbS/CdS core/shell CQD on TiO_2 nanowire solar cells.[21] In this paper, we describe the fabrication of a cascaded heterojunction photovoltaic device, utilizing a blend of 1.2 eV and 1.4 eV core/shell PbS/CdS CQDs, with an optimized thin film layer composition.

Shell thickness is estimated by a combination of UV-Vis absorption spectrometry, XRD, and XRD simulations and is based on the assumption that the CQDs are spherical. Details of this can be found in the supplementary material,[22] and in

a)Author to whom correspondence should be addressed. Electronic mail: Andrew.watt@materials.ox.ac.uk

our prior studies,[23] we have shown that optimum thickness of the CdS shells was ~0.1 nm, estimated by a combination of UV-Vis spectrometry and calculations. It must be noted that this value of shell thickness might be an underestimation of the actual thickness due to the assumption that the CQDs are perfectly spherical. 1.2 eV and 1.4 eV quantum dots were blended in solution and spin-cast on silane treated glass substrates for spectroscopic measurements. All films were 200 nm ± 17 nm thick: this is important for making direct comparisons of PL intensity. Photovoltaic devices were fabricated using CQD solutions at a concentration of 40 mg/ml in octane, and the blends were mixed at 1:1 ratio by volume. Structures were built upon patterned indium tin oxide (ITO) coated glass on which 50 nm of Poly(3,4-ethylenedioxythiophene): Polystyrene sulfonate (PEDOT:PSS) was spin coated. CQD layers were built up using 1,2-Ethandithiol (EDT) and cetyltrimethylammonium bromide (CTAB) dispersed in methanol to exchange ligands. The usage of CTAB[24] as a source of bromine (Br) ligand, and subsequently, the technique of hybrid passivation[25] (using both halide and organic ligands) have previously shown improved device performance by passivating the surface of CQDs and also improves charge mobility via doping. ZnO was prepared using the method described by Pacholski *et al.*[26] Full details of materials synthesis and device fabrication are given in the supplementary material.[22]

Photoluminescence can be used to understand energy transfer.[10,17] The PL spectra of the core and core/shell blends show only the emission from the larger quantum dots with peaks around 1140 nm and 1150 nm for Br + EDT-exchanged PbS/CdS and PbS CQD, respectively, as shown in Figure 1(a). This quenching effect of the larger band gap PL is not due to exciton dissociation or charge tunneling but rather a resonant energy transfer of exciton from the larger to smaller band gap CQD, thus also resulting in a rise in PL of the smaller band gap CQD (see Figure S1 (Ref. 22)).

The PL intensity of the core/shell blend emission is much greater than that of the core-only blend, implying that the shell reduces non-radiative recombination.[27] The PbS/CdS blends have a longer PL decay lifetime for both components, τ_1 and τ_2 (Figure 1(b)), compared to PbS blends, which again serves as an indicator of reduced carrier recombination through non-radiative processes.[28] The rate of the PL process is a sum of both radiative and nonradiative recombination rates, and PL lifetime is inversely proportional to this rate (Eq. (1)), hence any decrease in non-radiative recombination component would result in an increased PL lifetime[29]

$$\tau = \frac{1}{k_r + k_{nr}}, \tag{1}$$

where τ is the PL lifetime and k_r and k_{nr} are the radiative and nonradiative recombination rates, respectively. Further, increased PL lifetime has been shown to correlate with better material quality and device performance in other material systems.[30–33]

The current-voltage and external quantum efficiency (EQE) of both blends forming heterojunctions with ZnO are shown in Figures 1(c) and 1(d), respectively. For the purpose of this study, we utilized a 200 nm thick active layer and the power conversion efficiency of both devices is poor, reaching 2.4% for the core blend and 2.1% for the core/shell blend. We purposely make devices that are much thicker than the depletion width afforded by the heterojunction so as to demonstrate that quantum funneling does occur to alleviate the problems of a limited depletion width and contributes to charge extraction. Photogenerated charges outside of the depletion width may be funneled into it, thereby increasing the probability that they would be extracted. The EQE of the PbS/CdS device is worse than the PbS-only blend due to the lower J_{sc}. However, the PbS/CdS device has a more distinct excitonic band edge which could indicate improved preservation of quantum confinement. Photogenerated charges in PbS/CdS layer experience higher resistance[19] and lower mobility and with a 200 nm thick active layer, this impedes charge extraction, resulting in lower quantum efficiencies. However, to investigate the extent of carrier recombination

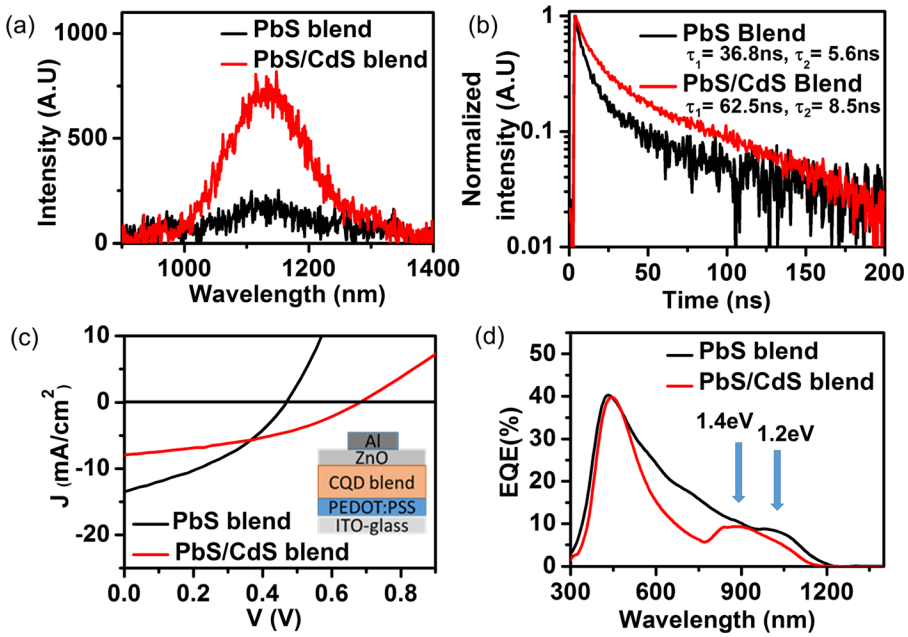

FIG. 1. (a) PL spectrum of CQD blend films on glass. Excitation source is a pulsed 505 nm laser head (5 MHz, 0.3 μJ/cm^2/pulse). (b) PL decay of PbS blend films and PbS/CdS blend films, taken at 1190 nm and 1140 nm, respectively. Lifetime was obtained from a bi-exponential fit. (c) *J-V* performance curve of blend devices which has a 200 nm thick layer of CQD blend films, topped with a ZnO layer. Inset depicts the device structure. (d) External quantum efficiency characterization of the devices described in (c). Arrows point to the first excitonic peak energy of 1.2 eV and 1.4 eV PbS and PbS/CdS CQD.

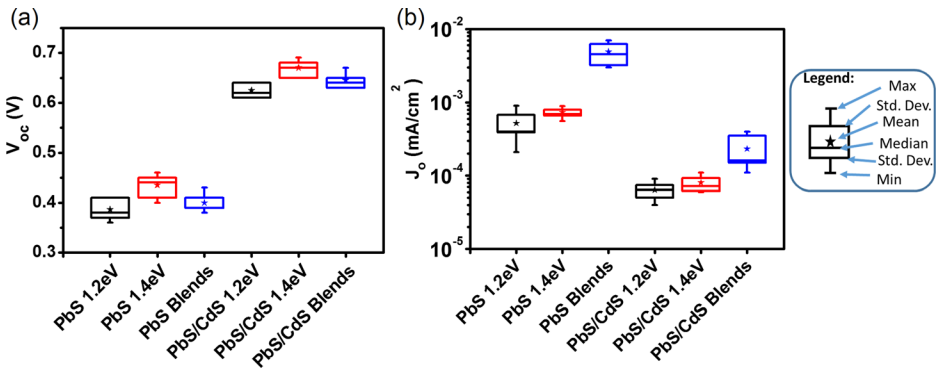

FIG. 2. (a) Open-circuit voltage and (b) reverse saturation current of devices fabricated with *n*-type ZnO layer on top of 200 nm PbS and PbS/CdS blends, respectively. Each sample statistic is built upon 18 devices, with 3 devices on each substrate.

(which is affected by trap densities), we turned to the open-circuit voltage and reverse saturation current of devices.

Figure 2 compares the open circuit voltage and reverse saturation current for single CQD materials and blends with and without shells. We hypothesize that resonant energy transfer is efficient from large to small band gap CQDs but the subsequent extraction of charges is dependent on the electric field created by the ZnO heterojunction or charge diffusion to an electrode. The success of charge extraction is reliant on charge transport efficiency which is in turn dependent on carrier recombination rates. Figure 2(b) shows that reverse saturation current, which is a good metric for recombination, is much lower in the PbS/CdS blend compared to the PbS blends, and that for both materials the reverse saturation current is greater in the case of the blend, compared to the corresponding single band-gap materials. Charge transport is impeded by trap states which can be thought of as (1) crystallographic defects on the surface of the CQD and (2) in a blend the small band gap CQD acts as a trap for the large band gap CQD, creating energy disorder.[17] Thus, devices comprising of blends, as compared to single-component systems, show a higher trap density (and higher recombination current). However, if we compare solely the devices comprising of CQD blends, PbS/CdS core/shell blends have lower recombination current compared to PbS blends as CdS presents itself as an epitaxial shell of larger band gap semiconductor material around the PbS cores, mitigating surface trap states. This idea is illustrated in Figure 3(a).

The next challenge is to further improve the core/shell blend device performance by modifying the device architecture. CQD solar cells rely heavily on the depletion zone to separate charges by drift because the innate disorder in nanocrystalline systems results in short carrier diffusion lengths.[34] Therefore, at high forward bias (for example, at the maximum power point), the depletion width is very much reduced and diffusive transport dominates, resulting in fewer charges being successfully extracted at the electrodes (refer to Figures 3(b) and 3(c)). This is reflected in the low fill factors observed for CQD solar cells.[35] A bilayer structure (Figure 3(d)) would fare better than the usual heterostructure due to a potential difference that serves as an electron blocking layer and also some amount of charge funneling at interfacial region between the 1.2 eV and 1.4 eV layers. To maximize the effect of funneling, a blend layer could be incorporated to improve the interfacial area so that charges can be cascaded very quickly from any 1.4 eV CQD to a neighboring 1.2 eV CQD, even without the presence of band bending or internal electric field from the depletion width. Improving charge transport at near flatband potential situations would help to improve device fill factor.

Assuming that the 1.2 eV CQD is well percolated throughout the blend as shown on TEM samples (see Figure S3 (Ref. 22)), funneled charges could follow a continuous pathway towards their respective electrodes. However, the charge transport of charges after the process of funneling is problematic. Based on the energy levels measured and calculated by Hyun *et al.*,[36] energy barriers will be formed between small band-gap CQD in the vicinity of large band-gap CQD, both at the HOMO and LUMO energy level states (Figure 3(a)). These could be overcome by the internal electric field provided by the band-bending effect of the

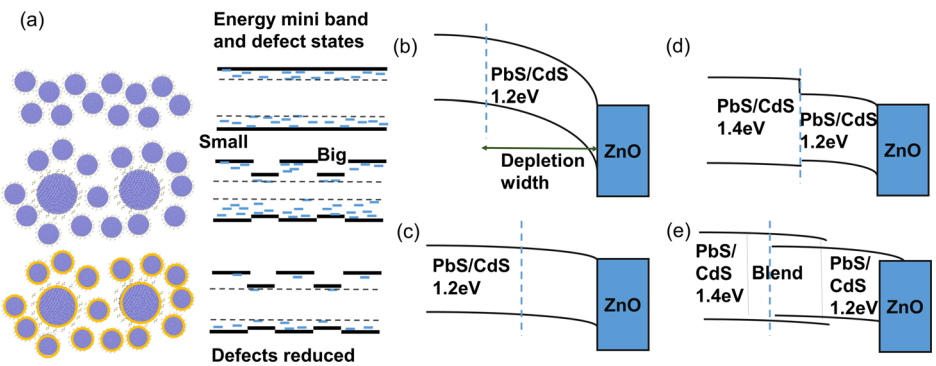

FIG. 3. (a) An illustration of mini band formation of pure phase PbS, the bimodal PbS blend, and the bimodal PbS/CdS blend. The CdS shell passivates surface states that form trap level states as compared to pure phase PbS such that charges funneled into the big (smaller band gap) quantum dots would be less likely to recombine. Band bending of heterostructure device (b) at short circuit current and (c) at forward bias, at maximum power point. Band bending, at maximum power point, of a (d) bilayer device and (e) blend device in "sandwich" configuration.

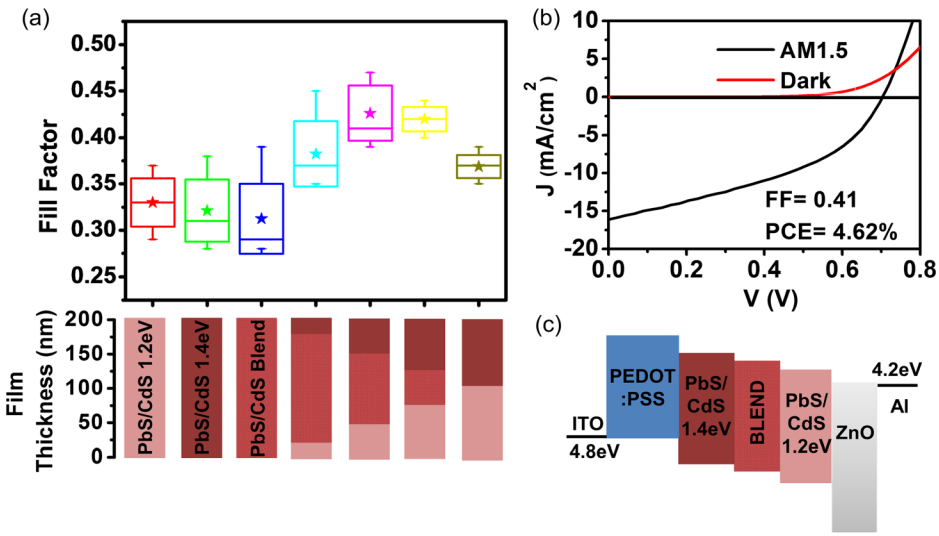

FIG. 4. (a) Fill factor recorded for devices fabricated with n-type ZnO layer on top of PbS/CdS CQDs and blends with various architectures. Total thickness of CQD film was fixed at 200 nm. Colors correspond to the components depicted in part. (c) Best fill factors were achieved with a 100 nm blend sandwiched between 1.2 eV and 1.4 eV PbS/CdS layers, each 50 nm thick. (b) Device performance of the champion cell made with this architecture. (c) Band alignment diagram of champion device.

TABLE I. Data statistics for heterojunction, full blend, sandwich configuration, and bilayer structure. Data are averaged over 36 devices across 12 separate substrates, with standard deviation reported. Refer to Figure 4(a) for the schematics of the individual structures. 1 blend 6L 1 refers to 25 nm of 1.2 eV PbS/CdS layer, 150 nm of blend layer and 25 nm of 1.4 eV PbS/CdS layer, etc.

Structures	PbS/CdS 1.2 eV	PbS/CdS 1.4 eV	PbS/CdS blend	1 blend 6L 1	2 blend 4L 2	3 blend 2L 3	PbS/CdS bilayer
J_{sc} (mA/cm^{-2})	8.9 ± 0.8	5.9 ± 1.8	6.8 ± 0.7	12.5 ± 2	14.3 ± 1.3	13.5 ± 1.2	11.8 ± 1.9
V_{oc} (V)	0.63 ± 0.02	0.68 ± 0.02	0.65 ± 0.02	0.66 ± 0.01	0.68 ± 0.02	0.68 ± 0.01	0.64 ± 0.02
FF	0.33 ± 0.02	0.32 ± 0.03	0.31 ± 0.04	0.38 ± 0.04	0.43 ± 0.03	0.42 ± 0.01	0.37 ± 0.01
PCE (%)	1.9 ± 0.4	1.3 ± 0.6	1.4 ± 0.3	3.1 ± 0.3	4.1 ± 0.3	3.9 ± 0.5	2.8 ± 0.5

heterojunction but the depletion width is limited, which calls for the need to optimize the thickness of the blend region. To harness the advantage of the funneling mechanism and not to be restricted by charge transport issues, layers of pure 1.2 eV and 1.4 eV PbS/CdS are used to act as electron collecting and electron blocking layers, respectively, in an effort to also reduce the blend layer thickness (Figure 3(e)). By keeping the entire CQD layer thickness constant, we vary the composition of layers from a completely blended film to a blend layer being sandwiched between 1.2 eV and 1.4 eV CQD films, and finally to a 1.2 eV and 1.4 eV bilayer, as illustrated in Figure 4(a). We found that the sandwich configurations gave better fill factors and with that, our optimum device (Figures 4(b) and 4(c)) gave us an efficiency of 4.62%, almost a threefold improvement over devices made of only 1.2 eV or 1.4 eV PbS/CdS CQD of the same thickness (see Figure S4 (Ref. 22) for EQE). The device performances of various device architectures are summarized in Table I.

A multi-band gap quantum cascade photovoltaic device has been demonstrated using a blend of PbS/CdS core/shell CQD with 1.2 eV and 1.4 eV band gap. The inclusion of a semiconductor shell around the core allows the formation of blended multi gap structures with improved device performance associated with a reduction in non-radiative recombination and charge funneling from large to small band gap CQD alleviating the problem of short carrier diffusion length. To further optimize the performance, a graduated structure of low gap-blend-wide gap CQDs was introduced and power conversion of up to 4.6% was achieved primarily by improvements of fill factor.

We acknowledge funding from EPSRC (Platform Grant No. EP/F048009/1). D.C.J.N. was funded by A*STAR, Singapore, with a National Science Scholarship (PhD) award. G.E. was funded from Oxford PV Ltd and EPSRC through a nanotechnology KTN.

[1]H. Fu and S.-W. Tsang, Nanoscale **4**, 2187 (2012).
[2]X. Lan, S. Masala, and E. H. Sargent, Nat. Mater. **13**, 233 (2014).
[3]I. J. Kramer and E. H. Sargent, Chem. Rev. **114**, 863 (2014).
[4]R. J. Ellingson, M. C. Beard, J. C. Johnson, P. Yu, O. I. Micic, A. J. Nozik, A. Shabaev, and A. L. Efros, Nano Lett. **5**, 865 (2005).
[5]W. R. Algar, H. Kim, I. L. Medintz, and N. Hildebrandt, Coord. Chem. Rev. **263–264**, 65 (2014).
[6]O. E. Semonin, J. M. Luther, and M. C. Beard, Mater. Today **15**, 508 (2012).
[7]J. J. Choi, W. N. Wenger, R. S. Hoffman, Y.-F. Lim, J. Luria, J. Jasieniak, J. A. Marohn, and T. Hanrath, Adv. Mater. **23**, 3144 (2011).
[8]X. Wang, G. I. Koleilat, J. Tang, H. Liu, I. J. Kramer, R. Debnath, L. Brzozowski, D. A. R. Barkhouse, L. Levina, S. Hoogland, and E. H. Sargent, Nat. Photonics **5**, 480 (2011).
[9]T. A. Klar, T. Franzl, A. L. Rogach, and J. Feldmann, Adv. Mater. **17**, 769 (2005).
[10]F. Xu, X. Ma, C. R. Haughn, J. Benavides, M. F. Doty, and S. G. Cloutier, ACS Nano **5**, 9950 (2011).
[11]I. J. Kramer, L. Levina, R. Debnath, D. Zhitomirsky, and E. H. Sargent, Nano Lett. **11**, 3701 (2011).
[12]K. Cnops, B. P. Rand, D. Cheyns, B. Verreet, M. A. Empl, and P. Heremans, Nat. Commun. **5**, 3406 (2014).
[13]A. J. Heeger, Adv. Mater. **26**, 10 (2014).
[14]A. K. Rath, M. Bernechea, L. Martinez, F. P. G. de Arquer, J. Osmond, and G. Konstantatos, Nat. Photonics **6**, 529 (2012).
[15]P. Guyot-Sionnest, J. Phys. Chem. Lett. **3**, 1169 (2012).
[16]K. W. Kemp, A. J. Labelle, S. M. Thon, A. H. Ip, I. J. Kramer, S. Hoogland, and E. H. Sargent, Adv. Energy Mater. **3**, 917 (2013).
[17]D. Zhitomirsky, I. J. Kramer, A. J. Labelle, A. Fischer, R. Debnath, J. Pan, O. M. Bakr, and E. H. Sargent, Nano Lett. **12**, 1007 (2012).

[18]M. J. Speirs, D. M. Balazs, H.-H. Fang, L.-H. Lai, L. Protesescu, M. V. Kovalenko, and M. A. Loi, J. Mater. Chem. A **3**, 1450 (2015).
[19]L.-H. Lai, L. Protesescu, M. V. Kovalenko, and M. A. Loi, Phys. Chem. Chem. Phys. **16**, 736 (2014).
[20]D. A. Wheeler, B. C. Fitzmorris, H. Zhao, D. Ma, and J. Zhang, Sci. China: Chem. **54**, 2009 (2011).
[21]B. A. Gonfa, H. Zhao, J. Li, J. Qiu, M. Saidani, S. Zhang, R. Izquierdo, N. Wu, M. A. El Khakani, and D. Ma, Sol. Energy Mater. Sol. Cells **124**, 67 (2014).
[22]See supplementary material at http://dx.doi.org/10.1063/1.4930144 for detailed nanocrystal synthesis and device fabrication, UV-vis-NIR and PL spectral response, and TEM images.
[23]D. C. J. Neo, C. Cheng, S. D. Stranks, S. M. Fairclough, J. S. Kim, A. I. Kirkland, J. M. Smith, H. J. Snaith, H. E. Assender, and A. A. R. Watt, Chem. Mater. **26**, 4004 (2014).
[24]J. Tang, K. W. Kemp, S. Hoogland, K. S. Jeong, H. Liu, L. Levina, M. Furukawa, X. Wang, R. Debnath, D. Cha, K. W. Chou, A. Fischer, A. Amassian, J. B. Asbury, and E. H. Sargent, Nat. Mater. **10**, 765 (2011).
[25]A. H. Ip, S. M. Thon, S. Hoogland, O. Voznyy, D. Zhitomirsky, R. Debnath, L. Levina, L. R. Rollny, G. H. Carey, A. Fischer, K. W. Kemp, I. J. Kramer, Z. Ning, A. J. Labelle, K. W. Chou, A. Amassian, and E. H. Sargent, Nat. Nanotechnol. **7**, 577 (2012).
[26]C. Pacholski, A. Kornowski, and H. Weller, Angew. Chem., Int. Ed Engl. **41**, 1188 (2002).
[27]H. Zhao, M. Chaker, N. Wu, and D. Ma, J. Mater. Chem. **21**, 8898 (2011).
[28]J. M. Pietryga, D. J. Werder, D. J. Williams, J. L. Casson, R. D. Schaller, V. I. Klimov, and J. A. Hollingsworth, J. Am. Chem. Soc. **130**, 4879 (2008).
[29]M. Maiberg and R. Scheer, J. Appl. Phys. **116**, 123711 (2014).
[30]A. Kanevce, D. H. Levi, and D. Kuciauskas, Prog. Photovoltaics Res. Appl. **22**, 1138 (2014).
[31]J. Chantana, D. Hironiwa, T. Watanabe, S. Teraji, K. Kawamura, and T. Minemoto, Sol. Energy Mater. Sol. Cells **130**, 567 (2014).
[32]C. Wehrenfennig, M. Liu, H. J. Snaith, M. B. Johnston, and L. M. Herz, APL Mater. **2**, 081513 (2014).
[33]S. D. Stranks, G. E. Eperon, G. Grancini, C. Menelaou, M. J. P. Alcocer, T. Leijtens, L. M. Herz, A. Petrozza, and H. J. Snaith, Science **342**, 341 (2013).
[34]D. Zhitomirsky, O. Voznyy, L. Levina, S. Hoogland, K. W. Kemp, A. H. Ip, S. M. Thon, and E. H. Sargent, Nat. Commun. **5**, 3803 (2014).
[35]N. Zhao, T. P. Osedach, L.-Y. Chang, S. M. Geyer, D. Wanger, M. T. Binda, A. C. Arango, M. G. Bawendi, and V. Bulovic, ACS Nano **4**, 3743 (2010).
[36]B.-R. Hyun, J. J. Choi, K. L. Seyler, T. Hanrath, and F. W. Wise, ACS Nano **7**, 10938 (2013).